Supplemental Information for "Wave-Induced Uplift on Elevated Bridge Decks: A 2D CFD Sensitivity Study of the AASHTO and Modified-Goda Design Equations"

Sandesh Lamsal, Ph.D., P.E., M.ASCE

This Supplemental Information accompanies the main manuscript. It contains the full modified-Goda primitive equations (Section 1), a localized in-sample descriptor of the CFD-to-Doyle ratio at the case-02 wave condition (Section 2), the cnoidal recompute of $\eta_{\max}$ at the shallow-water anchors (Section 3), the mesh statistics and solver settings (Section 4), and the notation table (Section 5). All observations are reported within the limitations of the present 2D incompressible OpenFOAM model documented in the main manuscript.

1 Modified-Goda Primitive Equations

The modified-Goda primitives used by the Doyle 2025 uplift formulation of the main manuscript, in the normal-incidence form adopted here ($\beta = 0$), are

$$\eta^* = 0.75\,(1 + \cos\beta)\,H_{\max} \;=\; 1.5\,H_{\max}, \tag{1}$$

$$p_1 = \tfrac{1}{2}(1 + \cos\beta)\,(\alpha_1 + \alpha_2\cos^2\beta)\,\gamma_w\,H_{\max} \;=\; (\alpha_1 + \alpha_2)\,\gamma_w\,H_{\max}, \tag{2}$$

$$p_3 = \alpha_3\,p_1, \tag{3}$$

where the Goda coefficients depend on the wavelength L and water depth h:

$$\alpha_1 = 0.6 + \tfrac{1}{2}\left[\frac{4\pi h/L}{\sinh(4\pi h/L)}\right]^2, \tag{4}$$

$$\alpha_2 = \min\left[\frac{h_b - d_s}{3h_b}\left(\frac{H_{\max}}{d_s}\right)^2,\ \frac{2\,d_s}{H_{\max}}\right], \tag{5}$$

$$\alpha_3 = 1 - \frac{h'}{h}\left[1 - \frac{1}{\cosh(2\pi h/L)}\right], \tag{6}$$

with h_b the water depth one significant wavelength offshore, d_s the depth at the base of the structure, and h' the depth at the base of the front wall (set $d_s = h' = h$ for the flat-bottom test section used here).

2 Fitted Geometry and Air-Gap Surface

This section presents a four-parameter localized descriptor $\beta(a^*, B/L)$ fitted to the present CFD observations at the case-02 wave condition ($H = 0.5$ m, $T = 3$ s, $d = 2.0$ m). It is reported here for transparency on the in-sample reading of the CFD-to-Doyle ratio across the geometry and air-gap axes simultaneously, and is not offered as a general-purpose recalibration of the modified-Goda equation.

The form is multiplicative,

$$F_{\text{uplift}}^{\text{corrected}} = \beta(a^*, B/L)\, F_{\text{uplift}}^{\text{Doyle}}, \tag{7}$$

with a separable surface

$$\beta(a^*, B/L) = 1 + A_{\text{pk}}\, \phi(B/L)\, \psi(a^*), \tag{8}$$

where the geometry kernel

$$\phi(B/L) = (B/L)\,(B_{\max}/L - B/L)_+ \tag{9}$$

vanishes at the slender limit and at the cross-over $B_{\max}/L$, and the air-gap kernel

$$\psi(a^*) = (1 + \alpha_{\text{sub}}\, |a^*|_-)\, \exp(-\gamma\, a_+^*) \tag{10}$$

applies an exponential decay above SWL ($a_+^* = \max(a^*, 0)$) and a linear correction below SWL ($|a^*|_- = \max(-a^*, 0)$). The four parameters were fitted by nonlinear least squares on $\log \beta_{\text{qs}}$ across the combined geometry and air-gap training points. The fitted values ($A_{\text{pk}} = 32.0$, $B_{\max}/L = 0.58$, $\gamma = 9.1$, $\alpha_{\text{sub}} = -0.67$) reproduce the in-sample CFD observations to RMSE 0.41 on β across the 9 training points and are shown in Fig. 1. The fit is in-sample at a single wave condition; out-of-sample generalization to other (H, T, d) combinations is identified as future work and is not claimed here.

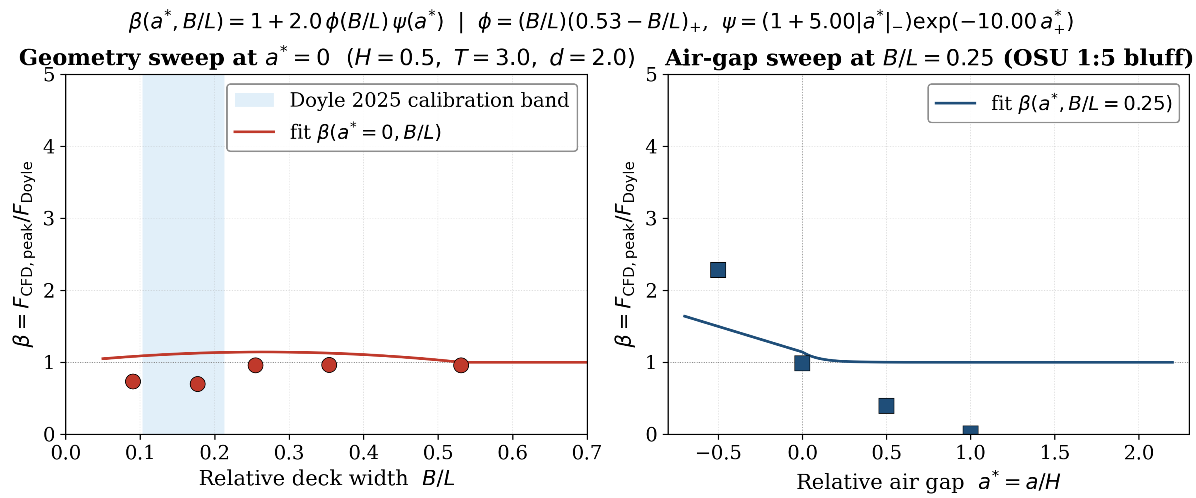

Figure 1: In-sample localized descriptor $\beta(a^*, B/L)$ fitted to the present CFD observations at the case-02 wave condition. Left: $\beta(B/L)$ at $a^* = 0$ across the seven B/L points, with the shaded band marking Doyle's calibration range. Right: $\beta(a^*)$ at the case-02 bluff $B/L = 0.255$. Markers are CFD observations; lines are the fitted surface. The fit is in-sample and is not intended for use across different (H, T, d) combinations.

3 Cnoidal Recompute of $\eta_{\max}$ at Shallow Anchors

At the Park 1:10 specimen anchors (cases 04 and 13, $d_{\text{local}} = 0.40$ m) the inlet Stokes-II wave model is used outside its conventional validity range. Table 1 recomputes the crest elevation $\eta_{\max}$ above SWL using first-order cnoidal theory (Wiegel 1964; Fenton 1979) and reports the multiplicative factor by which the CFD-to-Doyle quasi-static ratio shifts if the design-equation denominator is computed from cnoidal kinematics in place of Stokes-II.

Table 1: Cnoidal vs. Stokes-II $\eta_{\max}$ at the validation anchors and the intermediate-water case 02 baseline. The ratio-shift column is $(\eta_{\max,\mathrm{St-II}} - a)/(\eta_{\max,\mathrm{cn}} - a)$, the factor by which the published β_{qs} values would be multiplied if the design-equation $\eta_{\max}$ input were switched from Stokes-II to cnoidal. The intermediate-water case 02 is essentially unaffected; the shallow anchors are not.

Case	H [m]	T [s]	d [m]	kh	$\eta_{\max,\mathrm{St-II}}$ [mm]	$\eta_{\max,\mathrm{cn}}$ [mm]
Case 04 (Park 1:10)	0.18	3.72	0.40	0.348	226	148
Case 13 (Park 1:10)	0.50	3.91	0.40	0.330	1404	456
Case 02 (1:5 bluff)	0.50	3.00	2.00	1.111	289	271

For case 04 the multiplicative shift on β_{qs} is $226/148 = 1.53$, so the published CFD/Doyle$_{\mathrm{qs}}$ = 1.23 becomes ≈ 1.88 if cnoidal kinematics are used in the denominator. For case 02 the shift is $289/271 = 1.07$ and the ratios are essentially unchanged. The Stokes-II formula diverges in shallow water (the $\sinh^3(kh)$ denominator in the second-order crest shift goes to zero), which is why the case 13 Stokes-II $\eta_{\max}$ exceeds the water depth itself; this is the conventional signature that the wave theory has left its valid range. A cnoidal-inlet repeat of cases 04 and 13 is identified as future work in the Limitations section of the main manuscript.

4 Mesh Statistics and Solver Settings

The three production meshes used in the main manuscript (case 01 wave tank, case 02 bluff deck, case 03 I-girder deck) are summarized in Table 2. All three are two-dimensional, single-cell-thick, block-structured hex meshes generated by the multi-block `blockMesh` script with the deck cutout embedded directly in the background mesh. The wave tank uses a single uniform block; the bluff deck splits the domain into eight blocks around the rectangular cutout; the I-girder deck uses forty-one blocks resolving the six girder webs and bottom flanges. Every mesh passes `checkMesh` with zero average non-orthogonality and zero concave cells.

The production solver settings used for the bluff deck (case 02) are listed in Table 3. The same settings are used for case 03 and for every geometry, period, and air-gap program case, with the single exception of the GAMG-to-PCG switch on the pressure solver, which was made after the GAMG SIGFPE at the wave-impact spike.

5 Notation

The following symbols are used in the main manuscript:

A_{pk}	=	fitted peak-amplitude parameter of $\beta(a^*, B/L)$;
B	=	deck cross-shore base width (m);
$B_{\max}$	=	fitted cross-over deck width (m);
Co	=	Courant number;
$\mathrm{Co}_{\max}$	=	maximum Courant number permitted by the solver;
C_u	=	modified-Goda uplift coefficient;
$F_{\mathrm{CFD,peak}}$	=	per-step peak vertical force from CFD (N/m);
$F_{\mathrm{CFD,qs}}$	=	quasi-static envelope of vertical force from CFD (N/m);
F_{Doyle}	=	modified-Goda design uplift force (N/m);
F_{peak}	=	peak vertical force on the deck (N/m);

F_{qs} = quasi-static vertical force on the deck (N/m);
F_{uplift} = design uplift force per meter of spanwise length (N/m);
F_{vs}, F_{vh} = AASHTO vertical slamming and varying force components (N/m);
F_{hs}, F_{hv} = AASHTO horizontal slamming and varying force components (N/m);
F_x, F_z = horizontal and vertical integrated force on the deck (N/m);
$F_{1/250}$ = design statistic of irregular-wave force record (kN);
H = regular-wave height (m);
H_{max} = design-wave height (m);
H_s, $H_{1/3}$ = significant wave height (m);
$H_{4\sigma}$ = four-sigma estimator of irregular wave height (m);
L = linear-theory wavelength at the structure (m);
L_b = block length in `blockMesh` grading (m);
L_p = peak wavelength of the design spectrum (m);
T = wave period (s);
T_{dom} = dominant period extracted by FFT (s);
T_p = peak wave period of the design spectrum (s);
U = flow-velocity magnitude (m/s);
W_{deck} = spanwise deck width on which forces are integrated (m);
Z^* = inundation parameter, $(\eta_{max} - a)/H$;
a = air gap, measured upward from still-water level to the soffit (m);
a^* = relative air gap, a/H;
c = wave celerity (m/s);
c_{hs}, c_{hv} = AASHTO horizontal slamming and varying empirical coefficients;
c_r = AASHTO multi-girder force reduction factor;
c_{vs}, c_{vh} = AASHTO vertical slamming and varying empirical coefficients;
d = still-water depth (m);
g = gravitational acceleration (m/s^2);
h = water depth at the structure (m);
h_{deck} = total deck depth, top of slab to bottom of soffit (m);
h_{eff} = effective wave-engaged vertical projection of the deck (m);
k = wavenumber from the linear dispersion relation (1/m);
kh = relative depth;
n = cell count in a `blockMesh` block;
p = local soffit pressure (Pa);
p_1, p_3 = modified-Goda pressures at the still-water level and the bed (Pa);
p_5 = modified-Goda bottom-most horizontal pressure at the seaward face (Pa);
p_6 = modified-Goda leading-edge uplift pressure (Pa);
$p_{6,CFD}$ = CFD-resolved leading-edge soffit pressure (Pa);
q = per-cell geometric cell-size ratio in `blockMesh` grading;
r = end-to-end grading ratio in a `blockMesh` block;
t = time (s);
x, y, z = spatial coordinates of the 2D wave tank (m);
α = Volume-of-Fluid water-phase indicator;
α_{sub} = fitted submerged-deck parameter of $\psi(a^*)$;
β = CFD-to-design force ratio;
β_{peak} = per-step peak CFD-to-design ratio;
β_{qs} = quasi-static CFD-to-design ratio, $F_{CFD,qs}/F_{Doyle}$;
γ = exponential-decay parameter of $\psi(a^*)$;

γ_w	=	specific weight of water, $\rho_w g$ (N/m^3);
Δt	=	solver time step (s);
$\Delta x,\ \Delta z$	=	horizontal and vertical cell extents (m);
η	=	free-surface elevation above still-water level (m);
η^*	=	modified-Goda crest excursion (m);
$\eta_{\max}$	=	crest elevation above still-water level for the chosen wave theory (m);
ρ_w	=	water density (kg/m^3);
ϕ	=	geometry kernel of $\beta(a^*, B/L)$;
ψ	=	air-gap kernel of $\beta(a^*, B/L)$; and
ω	=	angular wave frequency, $2\pi/T$ (rad/s).

Table 2: Mesh statistics for the three reported cases. All meshes are 2D (single-cell-thick in y) and pass `checkMesh` with zero average non-orthogonality and zero concave cells. $\Delta x_{\mathrm{min}}, \Delta z_{\mathrm{min}}$ are the smallest cell extents over the whole domain. Wall-clock times are for a six-core domain decomposition on a single workstation.

Quantity	Case 01 (wave tank)	Case 02 (bluff)	Case 03 (I-girders)
Domain ($L_x \times L_z$) [m]	60×5	60×5	60×5
Blocks	1	8	41
Cells (2D)	75 000	103 360	163 968
Δx_{min} [mm]	100	96	19
Δx_{max} [mm]	100	102	100
Δz_{min} [mm]	17.5	9.2	9.2
Δz_{max} [mm]	169	84	46
Max aspect ratio	5.7	11.05	≤ 11
Max non-orthogonality [°]	0	0	0
Max skewness	$\sim 10^{-13}$	$\sim 10^{-13}$	$\sim 10^{-12}$
`deck` patch faces	—	92	506
Wall-clock to 20 s sim. [min]	~ 3	~ 6	~ 16

Table 3: Production `interFoam` solver settings for case 02.

Setting	Value
Solver application	`interFoam`
Pressure solver	PCG, DIC preconditioner
Velocity / scalar solver	smoothSolver / symGaussSeidel
α advection	Gauss vanLeer
α correction loops	2
α sub-cycles	1
PIMPLE outer correctors	1
PIMPLE pressure correctors	3
Maximum Courant number	0.3
Maximum α Courant number	0.3
Maximum Δt	0.005 s
Parallel decomposition	scotch, 6 subdomains
Wave generation BC	`waveVelocity`, Stokes II
Wave absorption BC	`shallowWaterAbsorption`